Ethenylene-bridged periodic mesoporous organosilicas: from *E* to *Z*

Carl Vercaemst,*, [a] Matthias Ide,[a] Paul V. Wiper,[b] James T. A. Jones,[b] Yaroslav Z. Khimyak,[b] Francis Verpoort[a] and Pascal Van Der Voort*, [a]

Electronic supporting information

Variable contact time (VCT) measurements have been used for studying the structure and dynamics of PMOs[1],polymer composites[2], and mesostrcutured alumino/silicas[3,4]. . Moreover, Jones *et al*[5]. have demonstrated the use of VCT measurements in conjunction with 2D heteronuclear correlation experiments (HECTOR) to determine the presence of structural heterogeneities in PMOs CP kinetics is measured by recording dependencies of signal intensity *vs.* contact time . The kinetic profiles can be fitted using different models.

'I-S Model' was derived for homogenous solids where the I-S heteronuclear dipolar interactions are relativity weak, whilst the I-I homonuclear dipolar interactions are strong enough to provide an efficient spin diffusion. For ^{1}H-^{13}C and ^{1}H-^{29}Si spin-½ systems, the I-S model is represented by equation (1):

$$I(t) = I_0\left(1 + \frac{T_{IS}}{T_{1\rho}^{S}} - \frac{T_{IS}}{T_{1\rho}^{I}}\right)^{-1}\left[\exp\left(-\frac{t}{T_{1\rho}^{I}}\right) - \exp\left(-t\left(\frac{1}{T_{IS}} + \frac{1}{T_{1\rho}^{S}}\right)\right)\right] \qquad (1)$$

Where I_0 is the absolute amplitude, $T_{1\rho}$ is the relaxation time in the rotating frame, T_{IS} is the CP time constant. For S spins, T_{IS} / $T_{1\rho}{}^{s}$ = 0, and the CP dynamics simplifies to:

$$I(t) = I_0\left(1 - \frac{T_{IS}}{T_{1\rho}^{I}}\right)^{-1}\left[\exp\left(-\frac{t}{T_{1\rho}^{I}}\right) - \exp\left(-\frac{t}{T_{IS}}\right)\right] \qquad (2)$$

The T_{IS} time constant is related to internuclear distances and molecular mobility. The $T_{1\rho}$ relaxation time describes the decay of intensity. T_{IS} is characteristic of chemical environment i.e. chemical groups containing additional I nuclei, such as $–CH_2$-CH_2-, result in faster T_{IS} values *cf.* –CH=CH- groups.

For framework-forming organic bridges we adopted an approach where two components with different T_{IS} and $T_{1\rho}{}^{H}$ times are identified depending on the mobility of the CP-determining ^{1}H source spins (Equation 3):

$$I(t) = I_0^{A}\left(1 - \frac{T_{IS}^{A}}{T_{1\rho}^{I}}\right)^{-1}\left[\exp\left(-\frac{t}{T_{1\rho}^{I}}\right) - \exp\left(-\frac{t}{T_{IS}^{A}}\right)\right] + I_0^{B}\left(1 - \frac{T_{IS}^{B}}{T_{1\rho}^{I}}\right)^{-1}\left[\exp\left(-\frac{t}{T_{1\rho}^{I}}\right) - \exp\left(-\frac{t}{T_{IS}^{B}}\right)\right] \qquad (3)$$

The 'fast' and 'slow' components ('A' and 'B') distinguish between surface bound bridges to that of bulk incorporated –CH=CH- functionalities, respectively.

Although the *I-S* model is simple to understand and is widely applied, it is not sufficient to describe the CP kinetics for solids with heterogeneous populations of the source spins. The *I-I**-

S model[6,7] takes into account the efficiency of spin diffusion, which relies on homonuclear dipolar interactions and proceeds through flip-flop spin transitions. Within this model, it is assume that the *I-S* heteronuclear dipolar interactions are strong enough in comparison to the *I-I* homonuclear dipolar interactions. Thus, the *I-I*-S* model relies on the existence of different *I* populations, denoted *I** for the *I* spins directly bound to an *S* spin under study and *I* for the rest of the *I* network. The CP proceeds in two steps. A fast rise of the intensity is observed initially due to the transfer of the magnetisation to a dilute spin (*I*-S)* by the abundant spins in close proximity followed by a slow rise of the intensity or damped oscillation. For long contact times, a decay of magnetisation or a plateau is observed.

Several equations have been proposed to describe the CP kinetics, the simplest is shown below (equation 2).[6]

$$I(t) = I_0 \exp\left(-\frac{t}{T_{1\rho}^{I}}\right)\left[1-\lambda\exp\left(-\frac{t}{T_{df}}\right)-(1-\lambda)\exp\left(-\frac{3}{2}\frac{t}{T_{df}}\right)\exp\left(-\frac{1}{2}\frac{t^2}{T_2{}^2}\right)\right] \quad (4)$$

where $T_{1\rho}^{I}$ is the *I* spin lattice relaxation time in the rotating frame; T_{df} is the ^{1}H spin-diffusion time constant describing the strength of the homonuclear dipolar interactions and the homogeneity of the *I* spin pool; λ is defined by the number *n* of *I* spins attached to the *S* spin under study ($\lambda = 1/(n+1)$); T_2 is the spin-spin relaxation time. Although the parameter T_2 needs to be fitted, due to its low value it has very little impact on the quality of the fitting.[6]

Ultimately, the applicability of the two models is subject to the homogeneity of the *I* spin population and depends on whether (*I-S* model) or not (*I-I*-S* model) the spin-diffusion is faster than the polarisation transfer from directly bonded I spins.

Structure of the pore walls

[SI1]
^{1}H-^{13}C CP/MAS kinetics

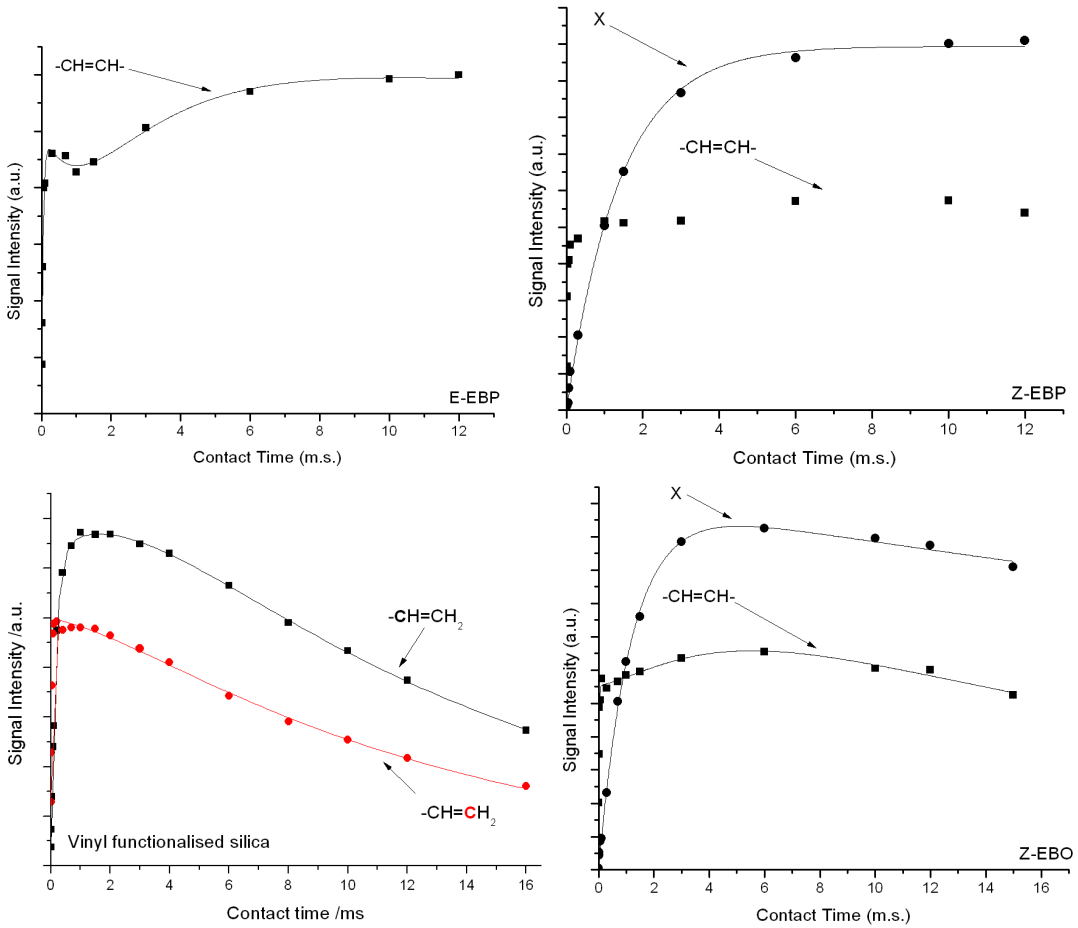

Figure S1: ^{1}H-^{13}C CP/MAS kinetic curves for E-EBP, Z-EBP, Vinyl functionalized silica and Z-EBO

Table S1: ^{1}H-^{13}C CP/MAS kinetic parameters for E-EBP, Z-EBP, Z-EBO and PMO-CH=CH_2 functionalised

Resonance	^{13}C Site	Model	Signal Intensity /10^7	T_{IS} /ms	$T_{1\rho}^{H}$ /ms	T_{df} /(m.s.)	T_2/(m.s.)	λ	R^2
E-EBP									
146.4	-CH=CH-	Fast	2.40 ± 0.011	0.05 ± 0.005	1.12 ± 0.38				0.990
	-CH=CH-	Slow	3.08 ± 0.450	2.09 ± 0.907	>100				
Z-EBP									
139.2	X	I-I*-S	1.0± 0.1	n/a	>100	1.45 0.05	0.001	0.99 ± 0.01	0.998
150.1	-CH=CH-	No $T_{1\rho}^{H}$	n/a	n/a	n/a				
Z-EBO									
139.2	X	I-I*-S	2.25 ± 0.05	n/a	75.9 ±13.0	1.25 ± 0.06	0.001	0.99 ± 0.01	0.998
150.9	-CH=CH-	Fast	0.98 ± 0.012	0.06 ± 0.004	1.46 ± 0.76				0.990
	-CH=CH-	Slow	1.42 ± 0.136	1.26 ± 0.15	>50				
PMO-CH=CH_2									
130.0	-CH=CH_2	Fast	5.94 ± 0.080	0.16 ± 0.004	2.58 ± 0.07				0.999
	-CH=CH_2	Slow	7.50 ± 0.024	2.53 ± 0.122	13.2 ± 0.81				
137.0	-CH=CH_2	Fast	4.90 ± 0.070	0.03 ± 0.001	1.69 ± 0.06				0.995
	-CH=CH_2	Slow	5.00 ± 0.200	1.74 ± 0.12	12.2 ± 0.95				

The results of the CP-kinetics for the peaks at 147 ppm for *E*-EBP and at 150 ppm for *Z*-EBP are consistent with our previous observations for framework forming organic bridges. Similarly to mono- and bifunctional –CH_2CH_2-/-CH=CH- PMOs[1, 5], we note that the ^{1}H-^{13}C CP/MAS kinetics curves give unsatisfactory results when fitted using either classical I-S or a more complex I-I*-S model relaying on the presence of heterogeneous ^{1}H population. This can only be explained using an approach where two components with different T_{IS} and $T_{1\rho}^{H}$ times are identified depending on the mobility of the CP-determining ^{1}H source spins (Table S1). The "rigid" component displays extremely short T_{cp} and $T_{1\rho}^{H}$ times and the "mobile" component shows much longer T_{cp} and $T_{1\rho}^{H}$ times. The fast CP of the rigid components is a result of directly attached protons with reduced mobility and is indicative of a strong ^{1}H-^{13}C heteronuclear dipolar coupled network, thus representing organic bridges embedded in the bulk of hybrid pore walls.

E-EBP exhibits short and long T_{IS} times' indicative of bulk and surface bound –CH=CH- bridges respectively. In an attempt to assign the resonance at *ca.* 139 ppm associated with the presence of Z-stereoisomer ^{1}H-^{13}C CP/MAS kinetic experiments were preformed: Due to the similarity in chemical shifts a vinyl-functionalised PMO was examined. Clearly, no similarity exists between that of the end =CH_2 group and the resonance *ca.* 139 ppm. The CP-kinetics for this peak for both Z-EBO and Z-EBP have been fitted using the I-I*-S model. The values of $\lambda > 0.9$ support the assumption that this lines represents a site with no directly attached protons.

Template-framework interactions

[SI2]
^{1}H-^{13}C CP kinetics of as-synthesized PMOs

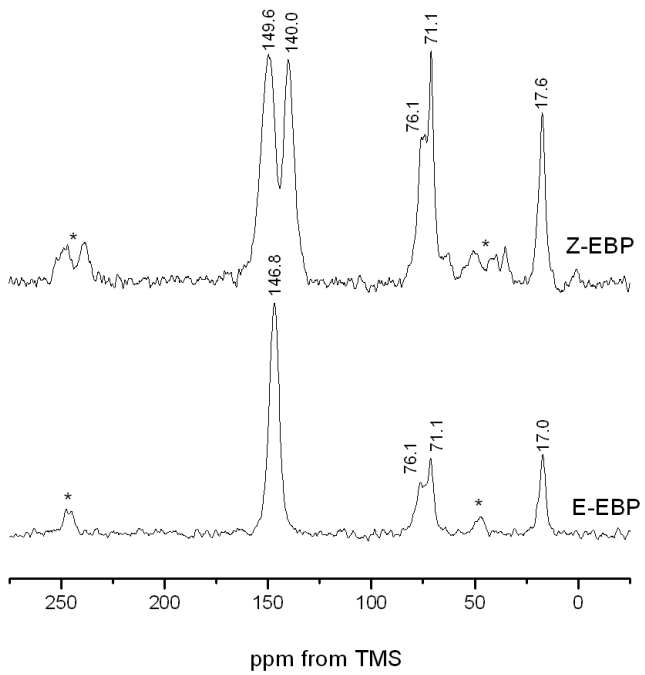

Figure S2: ^{1}H-^{13}C CP/MAS NMR spectra of E-EBP and Z-EBP as-synthesised PMOs acquired using a 1.5ms contact time and at an MAS rate of 8.0 kHz.

^{1}H-^{13}C CP kinetics of as-synthesized PMOs

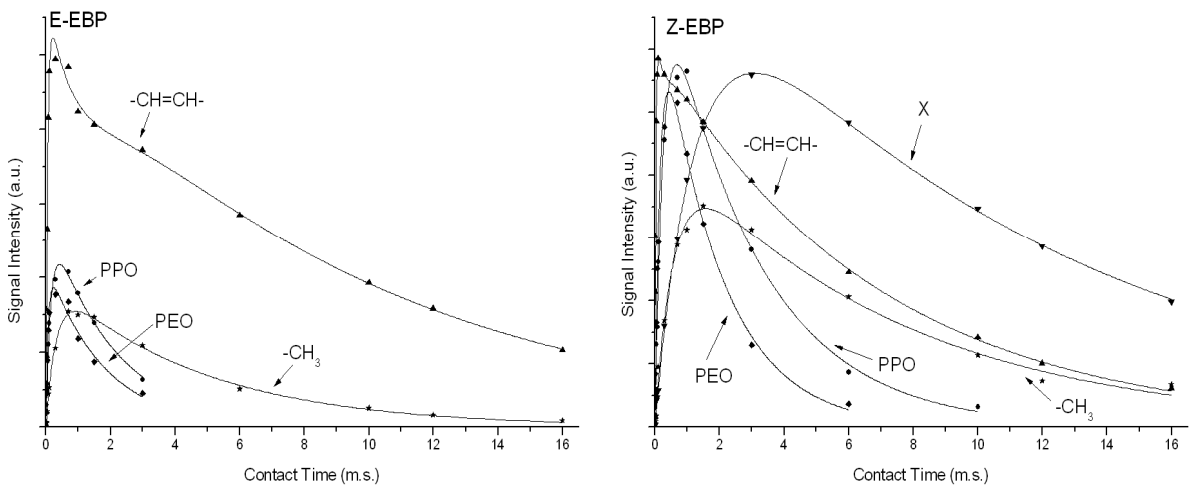

Figure S3: ^{1}H-^{13}C CP/MAS kinetic curves for E-EBP and Z-EBP

Table S2: ^{1}H-^{13}C CP/MAS kinetic parameters for E-EBP and Z-EBP respectively

Resonance	^{13}C Site	Component/ Model	Signal Intensity /10^7	T_{IS} /ms	$T_{1\rho}^{H}$ /ms	R^2
E-EBP						
17.0	$-CH_3$	I-S model	0.943 ± 0.02	0.32 ± 0.02	4.66 ± 0.25	0.994
71.1	PPO	I-S model	1.34 ± 0.086	0.15 ± 0.02	2.05 ± 0.29	0.974
76.1	PEO	I-S model	1.07 ± 0.057	0.07 ± 0.008	1.76 ± 0.21	0.969
146.8	-CH=CH-	Fast	2.76 ± 0.144	0.06 ± 0.007	0.84 ± 0.50	0.987
146.8	-CH=CH-	Slow	2.34 ± 0.186	1.17 ± 0.870	9.81 ± 1.67	0.987
Z-EBP						
17.6	$-CH_3$	I-S model	0.86 ± 0.040	0.57 ± 0.05	7.19 ± 0.49	0.987
71.1	PPO	I-S model	1.46 ± 0.052	0.26 ± 0.02	2.87 ± 0.22	0.992
76.1	PEO	I-S model	1.35 ± 0.060	0.16 ± 0.01	1.82 ± 0.16	0.988
140.0	X	I-S model	1.48 ± 0.030	1.24 ± 0.04	11.3 ± 0.39	0.998
149.6	-CH=CH-	Fast	1.14 ± 0.075	0.03 ± 0.003	0.21 ± 0.19	0.996
149.6	-CH=CH-	Slow	1.17 ± 0.025	0.25 ± 0.21	6.77 ± 0.31	0.996

^{1}H-^{13}C CP/MAS kinetic curves were fitted for the as-synthesised E-EBP and Z-EBP products. Kinetic parameters for the template resonances are fitted using a single exponential (I-S model) whilst the ethylene bridges are treated using double exponential. E/Z-EBP share similar T_{IS} and $T_{1\rho}^{H}$ times indicating that the template is held in a rigid geometry regardless of the isomeric configurations.

The ^{13}C resonance at *ca*. 71 ppm attributable to the PEO block of the template shows the fastest CP-kinetics in comparison with the peaks at of the PPO blocks. This is indicative of its restricted mobility due to location at the pore interface. The slower CP-kinetics of the peaks corresponding to the PPO blocks is due to their location in the middle of the pores.

Structure of pore walls

[SI3]
^{1}H-^{29}Si CP/MAS NMR kinetics

^{1}H-^{29}Si CP/MAS variable contact time experiments can be used to quantify the degree of condensation of the framework. The maxima of intensity in the ^{1}H-^{29}Si CP/MAS kinetics curves for each resonance correspond to the population of the specific sites and can be used for their quantification. The corresponding spectra featuring the optimum contact time can then be quantitatively deconvoluted using a Gaussian fit.

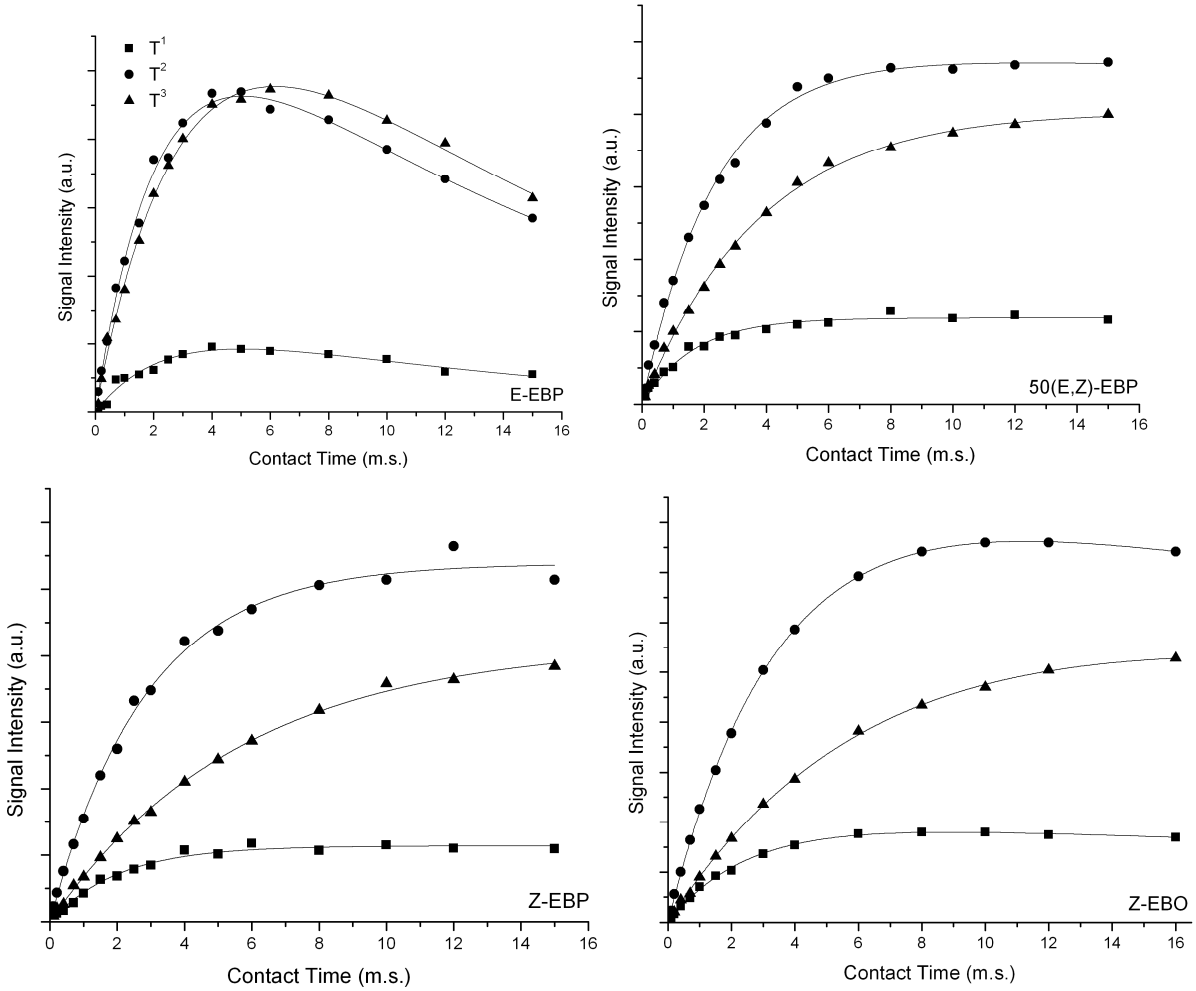

Figure S4: ^{1}H-^{29}Si CP/MAS kinetic curves of E-EBP, 50(E,Z)-EBP, Z-EBP and Z-EBO.

Table S3: ^{1}H-^{29}Si CP/MAS kinetic parameters for E-EBP, 50(E,Z)-EBP and Z-EBP respectively

Resonance	^{29}Si Site	Signal Intensity /10^7	T_{IS} /ms	/ms$T_{1\rho}^{H}$	R^2
E-EBP					
-64.8	-CH=CH- T^1	0.272 ± 0.0391	2.46 ± 0.53	12.80 ± 3.55	0.955
-74.6	-CH=CH- T^2	1.28 ± 0.0560	2.23 ± 0.15	15.54 ± 1.52	0.993
-83.2	-CH=CH- T^3	1.49 ± 0.0927	3.25 ± 0.27	13.90 ± 1.64	0.996
50(E,Z)-EBP					
-64.5	-CH=CH- T^1	0.60 ± 0.012	1.64 ± 0.11	>50	0.978
-72.1	-CH=CH- T^2	2.41 ± 0.088	2.32 ± 0.14	>50	0.997
-80.6	-CH=CH- T^3	2.05 ± 0.111	3.83 ± 0.29	>50	0.998
Z-EBP					
-62.1	-CH=CH- T^1	0.57 ± 0.0122	2.03 ± 0.13	-	0.983
-71.1	-CH=CH- T^2	2.70 ± 0.0390	2.82 ± 0.11	-	0.994
-78.9	-CH=CH- T^3	2.09 ± 0.0270	5.67 ± 0.15	-	0.999
Z-EBO					
-61.7	-CH=CH- T^1	1.00 ± 0.031	2.49 ± 0.13	>50	0.998
-71.3	-CH=CH- T^2	4.38 ± 0.061	3.41 ± 0.07	>50	0.998
-79.4	-CH=CH- T^3	3.24 ± 0.280	6.57 ± 0.65	>50	0.998

Degree of Framework Condensation:

[SI4]

Table S4: Degree of framework condensation calculated using the areas obtained under Gausian fitting acquired using contact time maxima of 16[a]/ 6[b]/12[c]ms

PMO	-cis loading (%)	$(T^1+T^2)/T^3$
E-EBP[b]	0	0.86
50(E,Z)-EBP[a]	50	1.49
Z-EBO[a]	100	1.65
Z-EBP[c]	100	1.42

Table S5: Degree of framework condensation calculated using the areas obtained under Gausian fitting, acquired using 2ms contact time

PMO	-cis loading (%)	$(T^1+T^2)/T^3$
E-EBP	0	1.37
80(E,Z)-EBP	20	1.68
50(E,Z)EBP	50	1.92
Z-EBP	100	2.53
Z-EBO	100	2.75

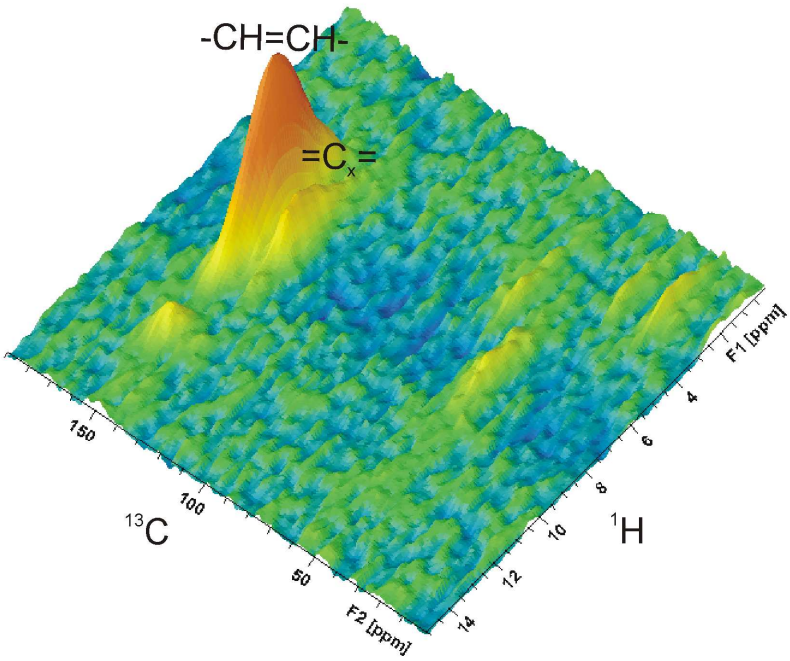

Figure S5: ^{1}H-^{13}C HECTOR NMR experiment of Z-EBO. The figure clearly illustrates both carbon environments coupled to the –CH=CH- protons. Low intensity cross-peaks correlate to residual template and $–OCH_3$ environments.

References

(1) Treuherz, B. A.; Khimyak, Y. Z. *Microporous and Mesoporous Materials* **2007**, *106*, 236-245.

(2) Luliucci, R.; Taylor, C.; Hollis, W. K. *Magnetic Resonance in Chemistry* **2006**, *44*, 375-384.

(3) Jones, M. D.; Duer, M. J. *Inorganica Chimica Acta* **2003**, *354*, 75-78.

(4) Khimyak, Y. Z.; Klinowski, J. *Physical Chemistry Chemical Physics* **2001**, *3*, 616-626.

(5) Jones, J. T. A.; Wood, C. D.; Dickinson, C.; Khimyak, Y. Z. *Chemistry of Materials* **2008**, *20*, 3385-3397.

(6) Kolodziejski, W.; Klinowski, J. *Chem. Rev.* **2002**, *102*, 613-628.

(7) Slabicki, M. M.; Potrzebowski, M. J.; Bujacz, G.; Olejniczak, S.; Olczak, J. *J. Phys. Chem. B* **2004**, *108*, 4535-4545.